Chapter VI

RESULTS AND DISCUSSION

Designing, characterization, and elucidation of mechanism of action of a peptide derived from the anticoagulant region of $NnPLA_2$-I enzyme,

&

assessment of *in vivo* toxicity, anticoagulant and antithrombotic activity of this anticoagulant peptide in a rodent model

Chapter VI

RESULTS AND DISCUSSION: Designing, characterization, and elucidation of mechanism of action of a 7-mer peptide from the anticoagulant region of $NnPLA_2$-I, and assessment of *in vivo* toxicity, anticoagulant and antithrombotic activity of this anticoagulant peptide in a rodent model

6.1 Brief Introduction:

Thrombin and FXa, the two key blood coagulation factors, have always been the most sought drug targets for development of antithrombotic and anticoagulant drugs [1-3]. A number of anticoagulant proteins and peptides showing inhibition of thrombin or FXa have been isolated and characterized from natural resources, snake venom included [4,5].

With recent advancement in technology, the application of peptides as therapeutics has significantly gained momentum [6-8]. To date, only two antiplatelet drugs have been successfully derived from disintegrins of viperid venom [9] and one bioactive peptide has been derived from *Agkistrodon acutus* venom hydrolysates with potential antithrombotic potency [10]. Although, a few 'synthetic anticoagulant peptides' have been developed from hirudin [11], no such attempt has been made from snake venom anticoagulant proteins.

In chapter IV, we have described the anticoagulant potential of $NnPLA_2$-I, a PLA_2 enzyme from *N. naja* venom, and it have been demonstrated that its anticoagulant activity is largely dependent on non-enzymatic inhibition of thrombin as well as by catalytic hydrolysis of plasma phospholipids. However, undesirable immune responses against protein therapeutics, resulting in reduced efficacy, anaphylaxis, and autoimmunity may be associated with direct application of snake venom PLA_2 enzyme (protein-based therapy) as an anticoagulant drug [12]. Therefore, in this chapter, a very low molecular weight anticoagulant peptide (MW, 775.85 Da) comprising of 7 amino acid residues (7-mer peptide) was designed by combining some of the thrombin-binding residues of $NnPLA_2$-I. The molecular mechanism of anticoagulant action of this synthetic peptide, its *in vivo* anticoagulant potency and pre-clinical safety was evaluated in a rodent model for its development into an anticoagulant drug prototype.

6.2 Results:

6.2.1 Design and synthesis of peptides corresponding to thrombin-binding regions of $NnPLA_2$-I

Based on the *in silico* analysis of $NnPLA_2$-I – thrombin interaction and pharmacological site of cobra venom PLA_2 [13,14], twelve anticoagulant peptides (ACR1 to ACR12) were designed (Table 6.1) and custom peptides were synthesized (GenPro Biotech, India).

6.2.2 Determination of physico-chemical properties of the synthesized peptides

The physico-chemical properties of the synthetic peptides determined by Expasy server are shown in Table 6.1.

Table 6.1. List of synthetic peptides designed from the thrombin binding region of $NnPLA_2$-I and their physico-chemical properties. The physico-chemical properties were determined by Expasy server, while ACE of interaction with thrombin was determined by ClusPro2.0 and Firedock servers.

Ref. ID	Peptide sequence	No. of residues	Charge at pH 7.0	MW (Da)	ACE* of THR binding
ACR1	AEKISGCWPYFKTYSYECSQGTLT	24	-0.1	2763.06	-261.60
ACR2	CYNEAEKISGCWPYFKTYSYECSQGTLTCKGD	32	-1.3	3676.06	-293.21
ACR3	AEKISECWDYFKTYSYECSQGTLT	24	-2.1	2853.10	-101.24
ACR4	AEGISGCWPYFGTYSYECSQGTLT	24	-2.1	2620.82	-152.35
ACR5	AEGISECWDYFGTYSYECSQGTLT	24	-4.1	2710.86	-205.14
ACR6	DKCSPKMILYSYKFHNGNIVCGDK	24	+2.0	2761.21	-222.31
ACR7	AGKMGCWPYFTLYKYKCSKGTLTC	24	+3.8	2750.29	-105.27
ACR8	AGKISGCWPYFKTYKYKCSKGTLT	24	+4.9	2731.20	-196.57
ACR9	EKISGGW	7	0.0	775.85	-224.28
ACR10	YFKT	4	+1.0	557.64	-
ACR11	EKISGGWGYFKT	12	+1.0	1372.52	-54.53

ACR12	EKISWYFKT	9	+1.0	1201.37	-25.14

*****atomic contact energy of peptide and thrombin as calculated by FireDock server.

6.2.3 Docking of ACR1-12 with thrombin

Docking analysis showed that all the peptides, except ACR10, have a strong interaction with thrombin with negative atomic contact energies (Table 6.1).

6.2.4 Screening of anticoagulant activity of ACR1-12

Among the 12 synthetic peptides, ACR9 (775.85 Da) demonstrated highest anticoagulant activity (Table 6.2). Further, the anticoagulant activity of ACR9 was found to be higher than that of heparin and argatroban; however, it showed less anticoagulant potency as compared to $NnPLA_2$-I (Table 6.2). Therefore, ACR9 was considered for further study.

Table 6.2. Re-calcification time (Unit) of mammalian platelet poor plasma (PPP) in presence of different concentrations (0.25 – 1.0 µM) of peptides (ACR1 to 12), $NnPLA_2$-I (0.25 – 1.0 µM), argatroban (0.25 – 1.0 µM), and heparin (0.25 – 1.0 µM). The clotting time of control PPP was recorded at 96.2 ± 3.1 s. Values are mean ± SD of triplicate determinations. Significance of difference in 'anticoagulant activity' as compared to $NnPLA_2$-I, *$p<0.05$; as compared to heparin, ‡$p<0.05$; and ¶$p<0.05$ as compared to argatroban.

Anticoagulant protein / peptide / drug	Anticoagulant activity (Unit)** at different concentrations of peptides (µM)			
	0.25	0.50	0.75	1.0
ACR1	0.2 ± 0.0	0.2 ± 0.0	0.3 ± 0.0	0.4 ± 0.0
ACR2	-6.2 ± 0.2	-6.5 ± 0.3	-2.8 ± 0.1	-0.5 ± 0.0
ACR3	-2.1 ± 0.1	-10.8 ± 0.9	-24.0 ± 1.2	-39.0 ± 2.0
ACR4	-1.5 ± 0.3	-3.6 ± 0.8	-8.2 ± 0.4	-12.0 ± 0.6
ACR5	-5.2 ± 0.2	-10.7 ± 1.0	-19.6 ± 1.0	-21.0 ± 1.1
ACR6	2.8 ± 0.8	1.1 ± 0.1	3.2 ± 0.2	4.4 ± 0.2
ACR7	0.5 ± 0.0	0.1 ± 0.0	0.8 ± 0.0	-0.3 ± 0.0
ACR8	-1.1 ± 0.1	0.7 ± 0.0	1.1 ± 0.1	-3.1 ± 0.2

ACR9	20.8 ± 1.1*‡¶	36.5 ± 2.5*‡¶	78.0 ± 1.9*‡¶	120.8 ± 1.6*‡¶
ACR10	0.1 ± 0.0	-0.8 ± 0.1	0.4 ± 0.0	0.3 ± 0.0
ACR11	-4.3 ± 0.8	-7.7 ± 0.9	-11.6 ± 0.8	-15.3 ± 0.8
ACR12	-3.2 ± 0.4	-3.8 ± 0.4	-8.2 ± 1.2	-11.2 ± 0.6
$NnPLA_2$-I	18.0 ± 1.0‡	61.0 ± 3.9‡	155.0 ± 2.4‡	217.0 ± 1.9‡
Heparin	10.2 ± 0.9*	29.0 ± 0.2*	42.8 ± 1.9*	51.9 ± 4.1*
Argatroban	11.1 ± 0.7*	29.8 ± 2.5*	69.3 ± 1.9*‡	85.1 ± 2.4*‡

**One unit of anticoagulant activity has been defined as peptide / $NnPLA_2$-I / heparin-induced 1 s increase in clotting time of the control PPP. Negative (-) sign in front of the values signify procoagulant activity.

6.2.5 Anticoagulant activity of ACR9

6.2.5.1 Effect of ACR9 on re-calcification time of whole blood and PPP

ACR9 dose-dependently prolonged the Ca-clotting time of mammalian whole blood (Fig 6.1A) and PPP (Fig 6.1B). The anticoagulant potency of ACR9 was found to be significantly higher ($p<0.05$) compared to commercial drug argatroban (Figs 6.1A, B).

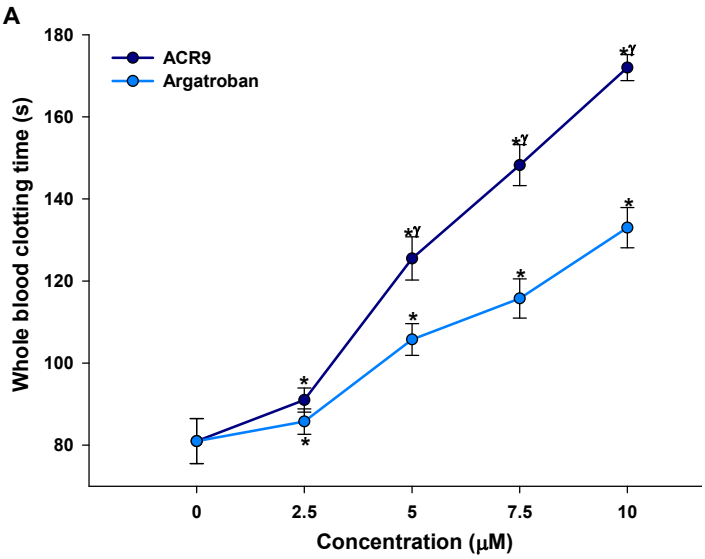

Fig 6.1A. Comparison of the dose-dependent effect of ACR9 (2.5 – 10.0 µM) and argatroban (2.5 – 10.0 µM) on whole blood clotting time. The clotting times of untreated (control) whole blood and PPP were recorded at 81.0 ± 5.5 s and 109.0 ± 4.2 s, respectively. Values are mean ± SD of triplicate determinations. Significance of difference *$p<0.05$ and $^{\gamma}p<0.05$ with respect to control and argatroban, respectively.

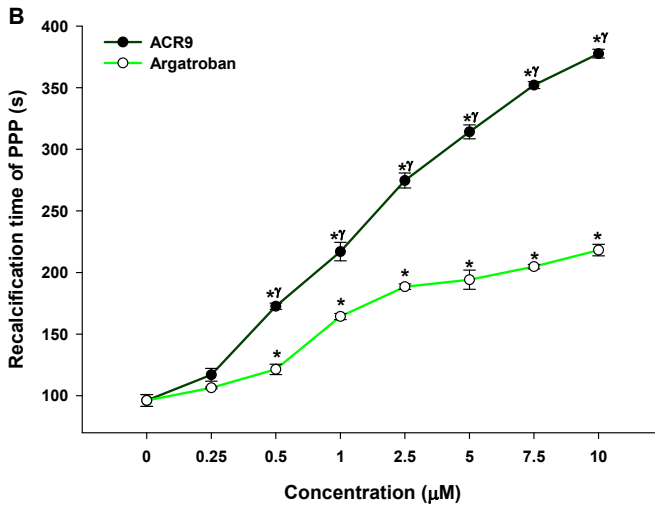

Fig 6.1B. Comparison of the dose-dependent effect of ACR9 (0.25 – 10.0 µM) and argatroban (0.25 – 10.0 µM) on re-calcification time of mammalian PPP. The clotting times of untreated (control) whole blood and PPP were recorded at 81.0 ± 5.5 s and 109.0 ± 4.2 s, respectively. Values are mean ± SD of triplicate determinations. Significance of difference *$p<0.05$ and $^{\gamma}p<0.05$ with respect to control and argatroban, respectively.

6.2.5.2 Effect of ACR9 on PT, APTT, and TT of PPP

ACR9 dose-dependently enhanced the PT, APTT, and TT of PPP; however, beyond a concentration of 1.0 µM, ACR9 had no further effect on APTT (Fig 6.2).

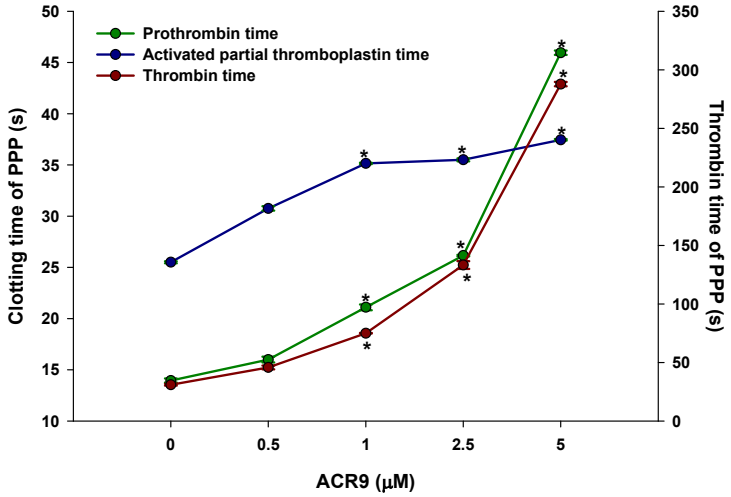

Fig 6.2. Dose-dependent (0.5 – 5.0 µM) effect of ACR9 on prothrombin time (PT), activated partial thromboplastin time (APTT), and thrombin time (TT) of PPP.

Values are mean ± SD of triplicate determinations. Significance of difference *p<0.05 with respect to control.

6.2.6 Thrombin inhibition by ACR9

6.2.6.1 Effect on fibrinogen clotting time of thrombin

ACR9 showed significantly higher (p<0.05) inhibition of thrombin against its physiological substrate fibrinogen as compared to argatroban (Fig 6.3A). Further, ACR9 time-dependently increased the fibrinogen clotting time of thrombin; albeit, post 20 min of pre-incubation of ACR9 with thrombin no further inhibition of thrombin was observed (Fig 6.3B).

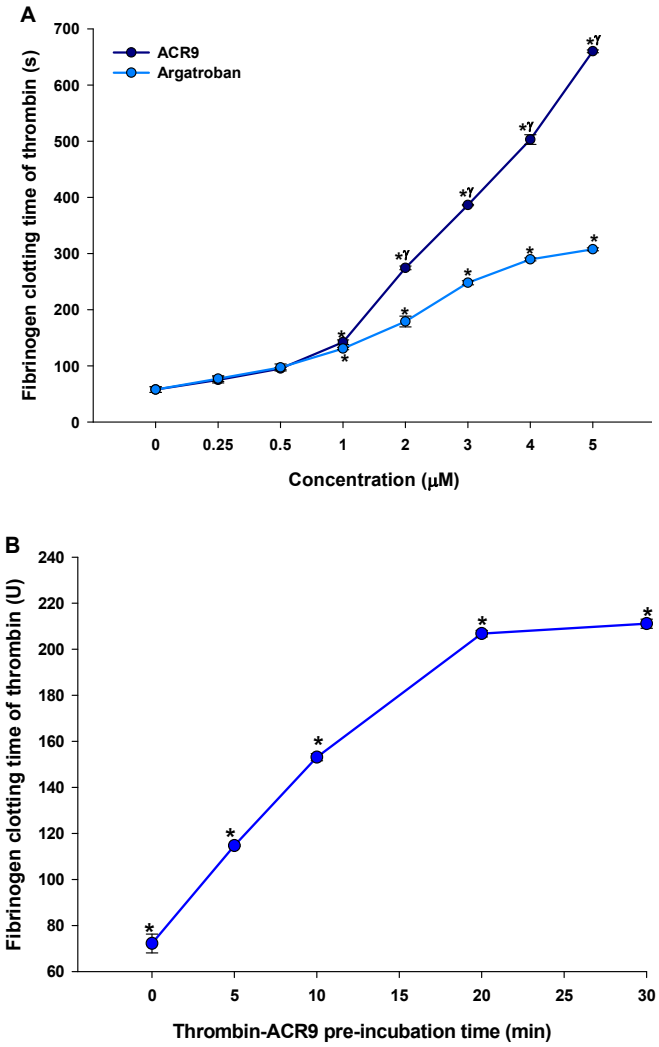

Fig 6.3. Effect of ACR9 on fibrinogen clotting time of thrombin. A. Dose-dependent (0.25 – 5.0 µM) effect of ACR9 and argatroban on the fibrinogen clotting time of

thrombin. Different concentrations of ACR9 / argatroban was incubated with 3 µl of 10 NIH units of human thrombin for 30 min at 37 ºC and the clotting time was recorded after adding 40 µl of 2.5 mg/ml fibrinogen. **B.** Time-dependent (0 – 30 min) effect of ACR9 (2.0 µM) on the fibrinogen clotting time of thrombin. ACR9 was incubated with 3 µl of 10 NIH units of thrombin for different time intervals at 37 ºC and the clotting time was then measured, as mentioned above. The clotting time of the fibrinogen incubated with thrombin was recorded at 57.8 ± 5.0 s. Values are mean ± SD of triplicate determinations. Significance of difference *$p<0.05$ and $^{\gamma}p<0.05$ with respect to control and argatroban, respectively.

6.2.6.2 Effect on amidolytic activity of thrombin

The dose-dependent inhibition of amidolytic activity of thrombin by ACR9 (Fig 6.4A) was found to be superior ($p<0.05$) as compared to argatroban (Fig 6.4B). From the log [inhibitor concentration] vs response curves, the IC_{50} value of thrombin inhibition by ACR9 and argatroban was determined at 2.00 ± 0.12 µM (Fig 6.4C) and 2.18 ± 0.13 µM (Fig 6.4D), respectively.

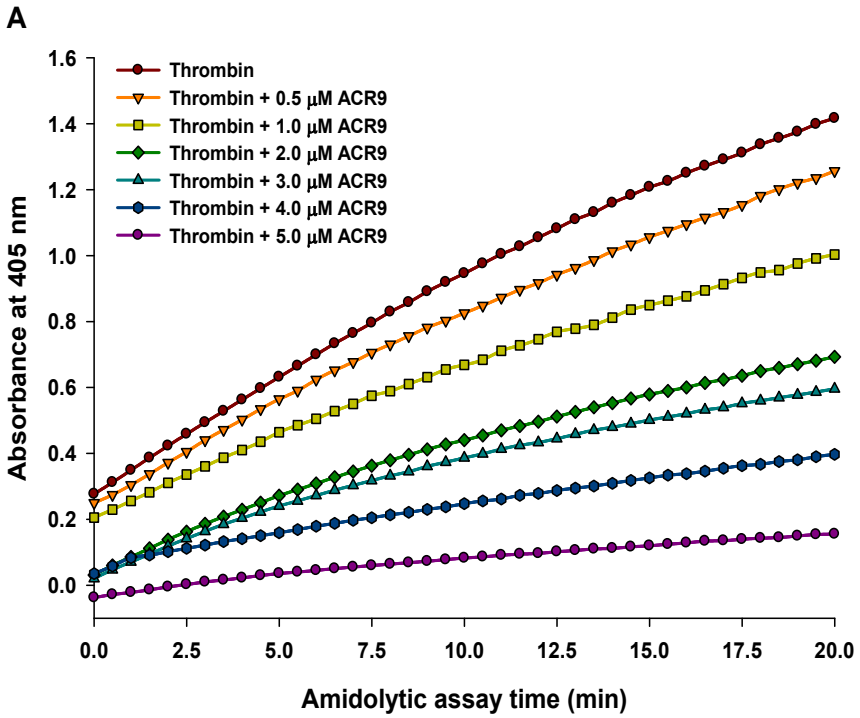

Fig 6.4A. Effect of ACR9 on amidolytic activity of thrombin. Dose-dependent (0.5 – 5.0 µM) effect of the ACR9 on the amidolytic activity of thrombin against its

chromogenic substrate N-(*p*-Tosyl)-Gly-Pro-Arg-*p*-nitroanilide acetate salt (0.2 mM). The kinetics (absorbance) of the reactions was measured up to 20 min at 405 nm.

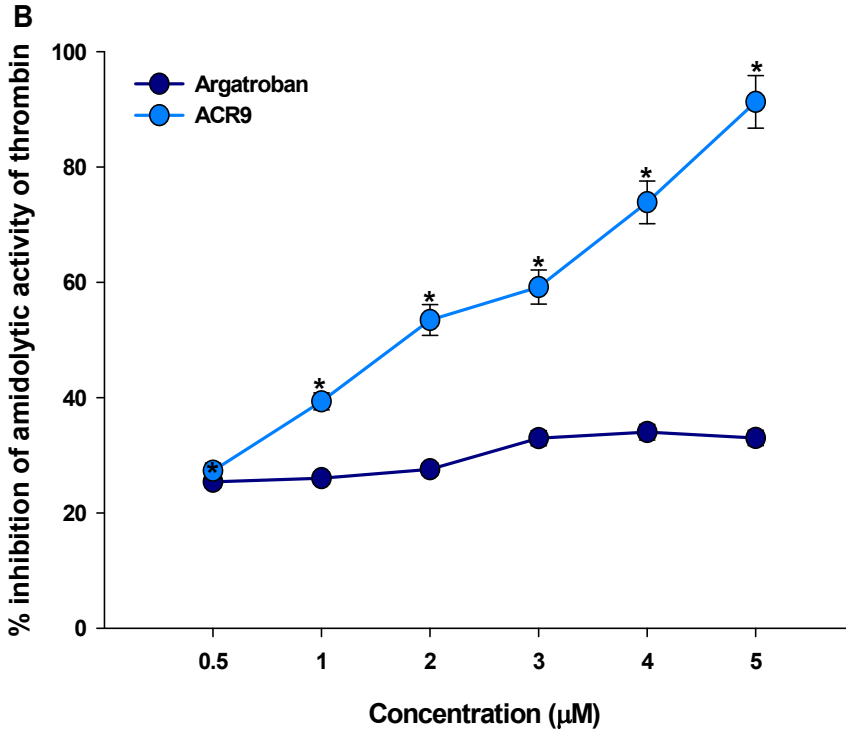

Fig 6.4B. Effect of ACR9 on amidolytic activity of thrombin (contd.). Dose-dependent (0.5 – 5.0 µM) inhibition of the amidolytic activity of thrombin by ACR9 and argatroban. Values are mean ± SD of triplicate determinations. Significance of difference *p<0.05 with respect to argatroban.

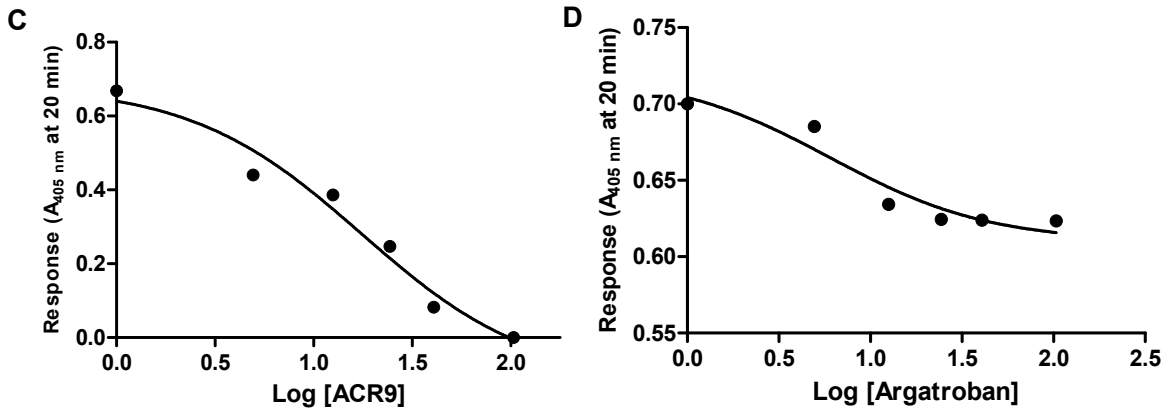

Fig 6.4. Log [inhibitor] vs response (absorbance at 405 nm) plot to determine the IC_{50} of thrombin inhibition by C. ACR9 and D. argatroban, respectively.

6.2.6.3 Kinetics of thrombin inhibition by ACR9

With increase in the concentration of inhibitor (ACR9), the amidolytic activity of thrombin showed a decrease in *Vmax* and increase in *Km* values (Table 6.3). Therefore, ACR9 showed mixed mode of thrombin inhibition with a *Ki* value of 0.39 ± 0.01 µM (Fig 6.5).

Table 6.3. Kinetics of inhibition of thrombin by ACR9. The kinetic parameters (*Km* and *Vmax*) were determined from the Michaelis-Menten plot as described in section 3.2.8.1.3 of chapter III. The values are mean ± SD of triplicate determinations.

ACR9 (µM)	*Vmax* (µmol *p*-NA released/min)	*Km* (mM)
0	13.88 ± 0.65	0.056 ± 0.001
10	8.12 ± 0.99	0.102 ± 0.002
20	6.10 ± 0.27	0.195 ± 0.002

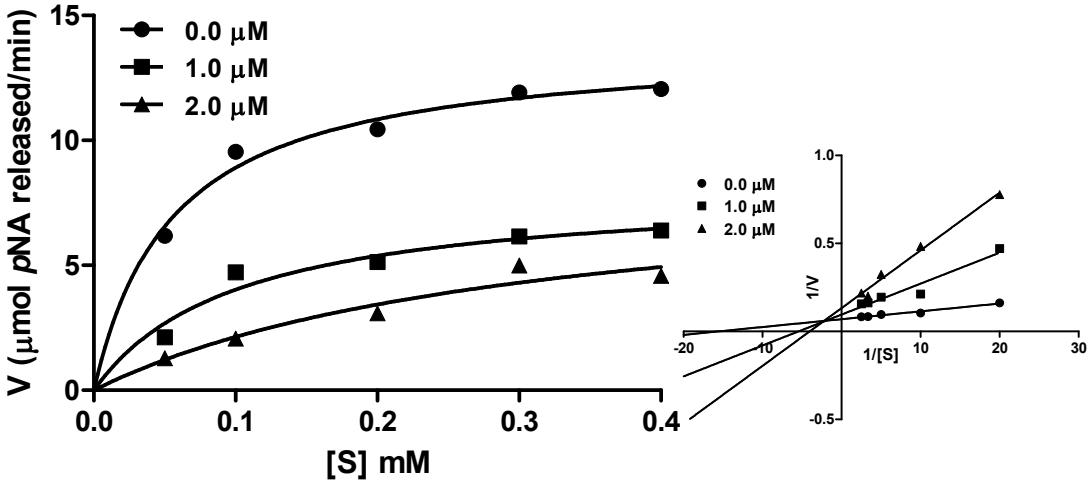

Fig 6.5. Michaelis-Menten plot to determine the kinetics of thrombin inhibition by ACR9 at 1.0 and 2.0 µM concentrations; goodness of fit of the plot, $R^2 = 0.99$. **Inset:** Lineweaver-Burk plot of the amidolytic activity of thrombin in absence and presence of ACR9 (1.0 and 2.0 µM); goodness of fit of the plot, $R^2 = 0.99$.

6.2.7 Factor Xa inhibition by ACR9

6.2.7.1 Effect on prothrombin activation by FXa

ACR9 dose-dependently inhibited the prothrombin activation property of FXa (Fig 6.6A), thereby inhibiting thrombin formation (Fig 6.6B).

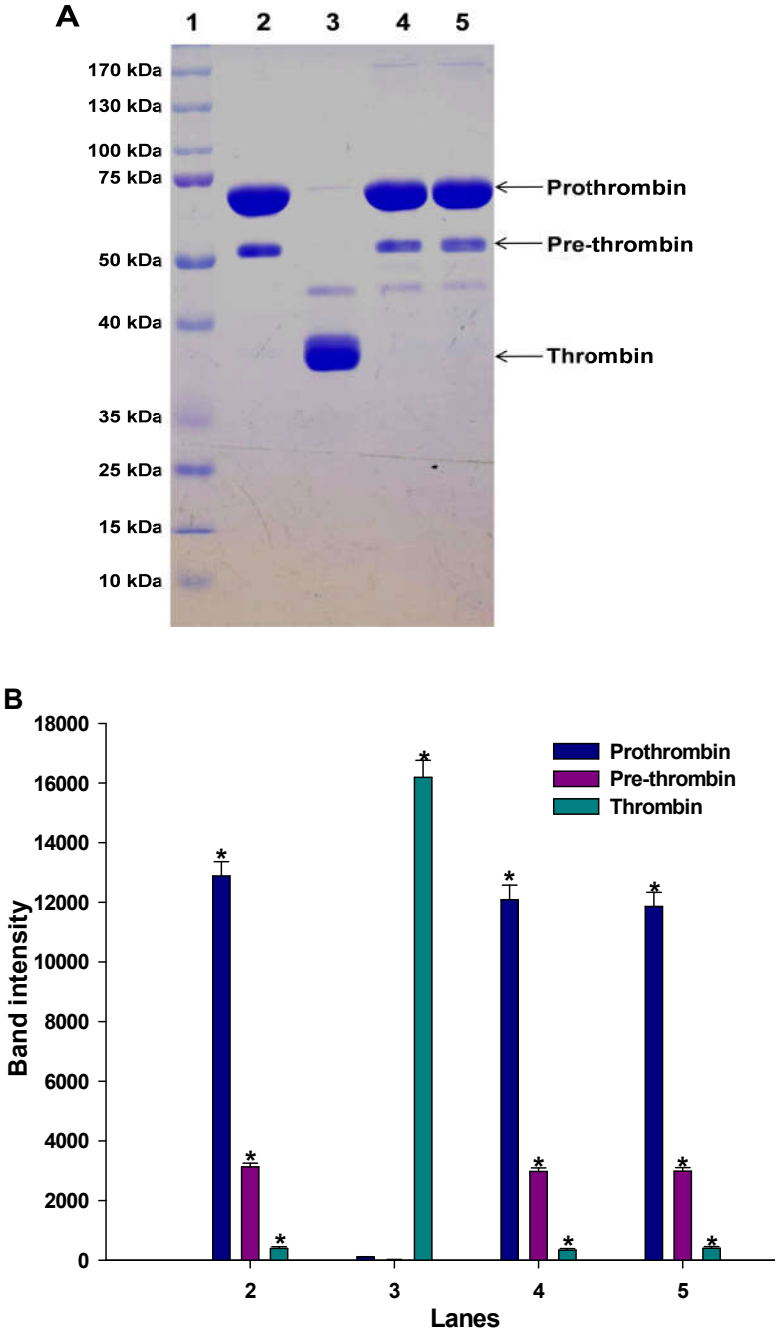

Fig 6.6. Effect of ACR9 on prothrombin activation by factor Xa. A. 12.5% SDS-PAGE analysis to determine the effect of ACR9 (1.0 and 2.0 µM) on the prothrombin

activation property of factor Xa (0.1 µg). Lane 1, protein molecular weight markers; lane 2, only prothrombin (12 µg); lane 3, prothrombin (12 µg) incubated with FXa (0.1 µg); lane 4, prothrombin (12 µg) incubated with ACR9 (1.0 µM) treated FXa (0.1 µg); lane 5, prothrombin (12 µg) incubated with ACR9 (2.0 µM) treated FXa (0.1 µg). **B.** Area of the protein bands of lanes 2-5 as determined by densitometry scanning using ImageJ software.

6.2.7.2 Effect on amidolytic activity of FXa

ACR9 dose-dependently inhibited the amidolytic activity of FXa against its chromogenic substrate F3301 (Figs 6.7A, B). From the log [inhibitor concentration] vs response curve, the IC_{50} value of FXa inhibition by ACR9 was determined at 19.6 ± 1.2 µM (Fig 6.7C).

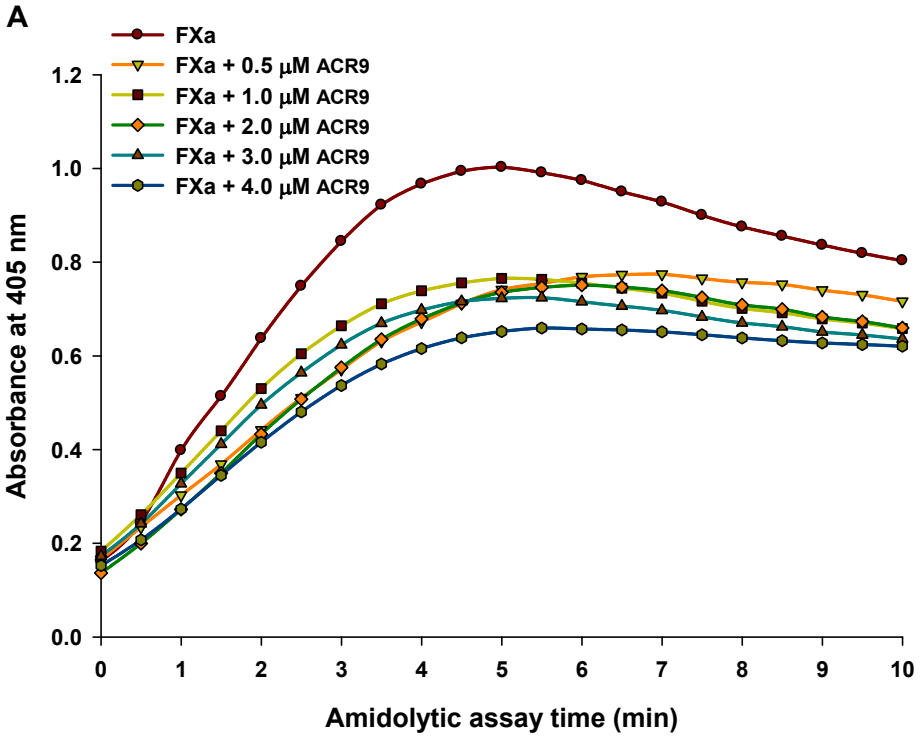

Fig 6.7A. Effect of ACR9 on amidolytic activity of factor Xa. Dose-dependent (0.5 – 4.0 µM) effect of ACR9 on the amidolytic activity of FXa against its chromogenic substrate CH_3OCO-D-CHA-Gly-Arg-*p*-NA-AcOH (0.2 mM). The kinetics (absorbance) of the reactions was measured up to 10 min at 405 nm.

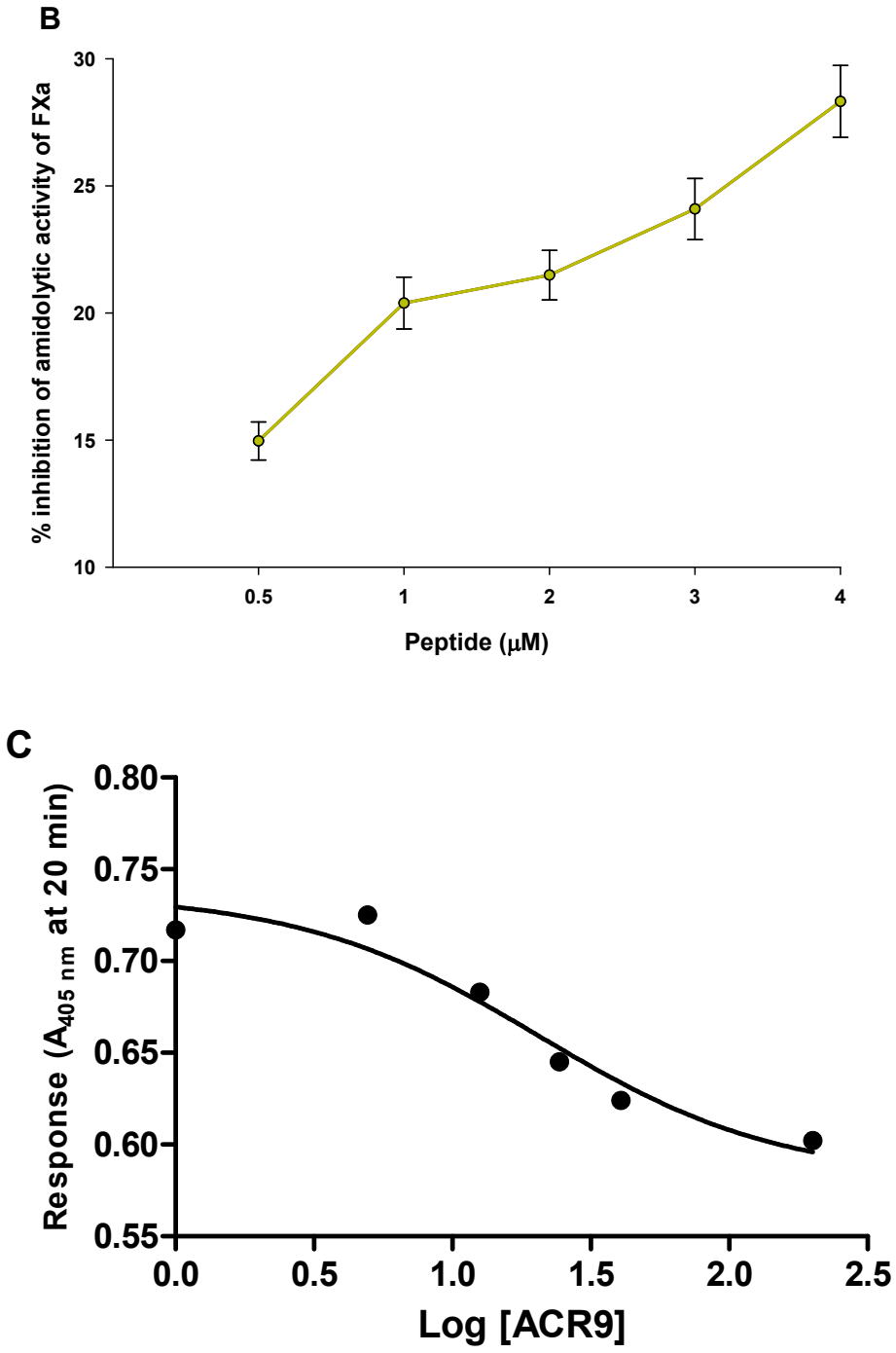

Fig 6.7. Effect of ACR9 on amidolytic activity of factor Xa (contd). B. Dose-dependent inhibition of the amidolytic activity of thrombin by ACR9 (0.5 – 4.0 μM). Values are mean ± SD of triplicate determinations. **C.** Log [ACR9] (peptide concentration) vs response (absorbance at 405 nm) plot to determine the IC_{50} of FXa inhibition by ACR9.

6.2.7.3 Kinetics of FXa inhibition by ACR9

Both *Vmax* and *Km* values of amidolytic activity of FXa were found to decrease with an increase in concentration of the peptide inhibitor (ACR9) (Table 6.4). Therefore, ACR exhibited uncompetitive inhibition of FXa (Fig 6.8), with an *αKi* value of 1.0 ± 0.2 µM.

Table 6.4. Kinetics of inhibition of factor Xa by ACR9. The kinetic parameters (*Km* and *Vmax*) were determined from the Michaelis-Menten plot as described in section 3.2.8.2.3 of chapter III. The values are mean ± SD of triplicate determinations.

ACR9 (µM)	*Vmax* (µmol *p*-NA released/min)	*Km* (mM)
0	55.93 ± 7.22	0.81 ± 0.05
10	33.32 ± 6.27	0.48 ± 0.01
20	13.47 ± 0.76	0.15 ± 0.02

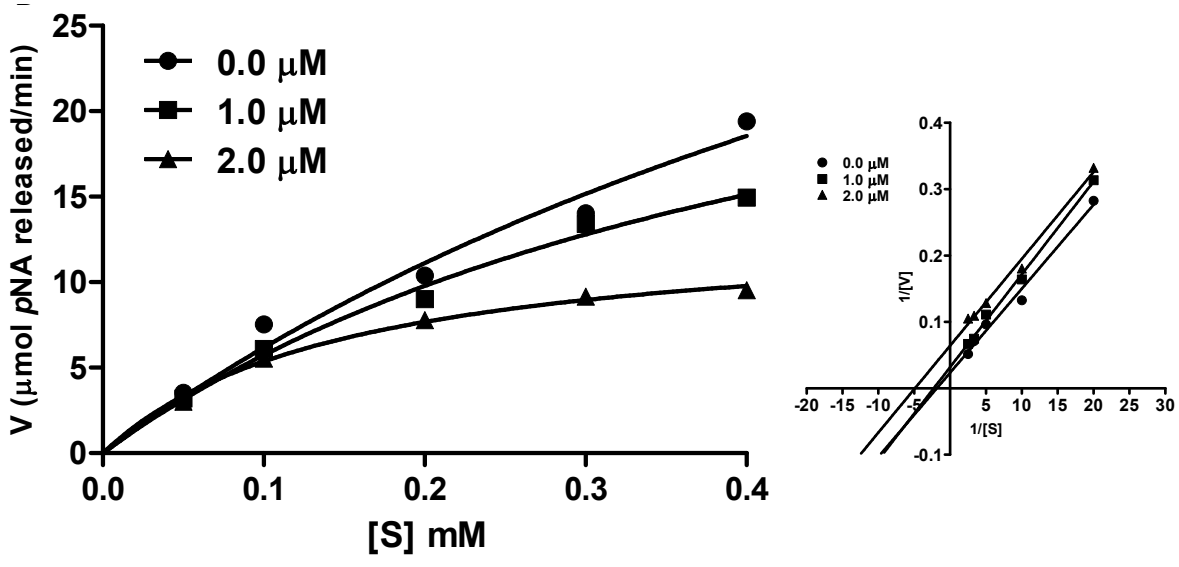

Fig 6.8. Michaelis-Menten plot to determine the kinetics of FXa inhibition by ACR9 (1.0 and 2.0 µM); goodness of fit of the plot, $R^2 = 0.97$. **Inset:** Lineweaver-Burk plot of the amidolytic activity of FXa in absence and presence of ACR9 (1.0 and 2.0 µM); goodness of fit of the plot, $R^2 = 0.99$.

However, pre-incubation of ACR9 (1.0 µM) with prothrombin for 30 min did not inhibit the prothrombin activation property of FXa (Fig 6.9).

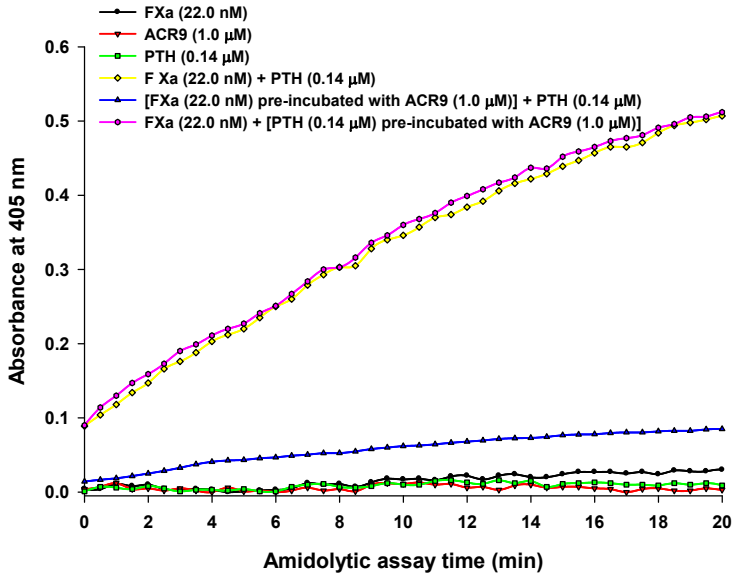

Fig 6.9. Effect of ACR9 on prothrombin as assayed by amidolytic assay of prothrombin activation by FXa against the chromogenic substrate of thrombin, N-(*p*-Tosyl)-Gly-Pro-Arg-*p*-nitroanilide acetate salt (0.2 mM). The kinetics (absorbance) of the reactions was measured up to 15 min at 405 nm.

6.2.8 Analysis of *in silico* binding of ACR9 to thrombin and FXa

6.2.8.1 Determination of structure of ACR9

The best structure of ACR9 was predicted with a peptide energy of -3.23 (Fig 6.10), and this model was docked with thrombin and FXa to understand the peptide-protein (thrombin / FXa) interaction.

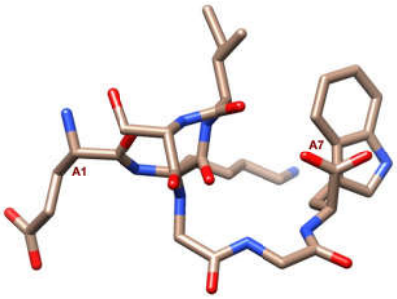

Fig 6.10. Best predicted structure for ACR9 by the PEPFOLD-3 Peptide Structure Prediction online web server.

6.2.8.2 Docking of ACR9 with thrombin

Docking of ACR9 with thrombin (Fig 6.11A) followed by Ligplot analysis showed that the peptide interacted with thrombin through 116 non-bonded contacts and 9 H-bond (Fig 6.11B). Contact map analysis suggested that 7 residues of ACR9 interacted with 19 residues of the heavy chain of thrombin with an atomic contact energy (ACE) and global energy (GE) of -224.28 and -38.4, respectively (Fig 6.11C). Interestingly, ACR9 showed binding with His57 and Ser195 residues of the catalytic triad of thrombin that can be correlated to the *in vitro* inhibition of the catalytic (amidolytic) activity of thrombin (Figs 6.11B, C).

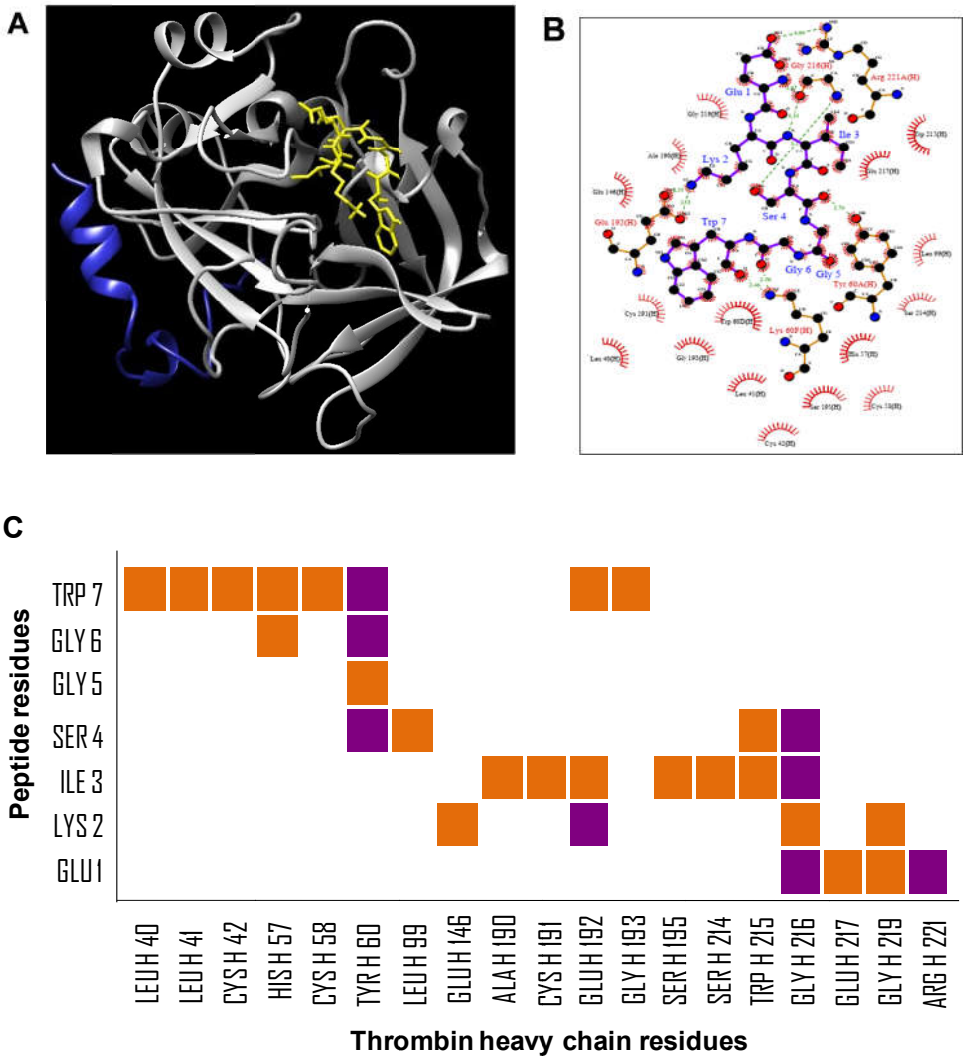

Fig 6.11. Docking of ACR9 with thrombin. A. Best docking model of ACR9 with thrombin (PDB ID: 3RM2) as predicted by the ClusPro 2.0 web server; yellow, grey,

and blue chains represent ACR9, heavy (H) chain, and light (L) chain of thrombin, respectively. **B.** Ligplot analysis to show the residue-to-residue interaction of ACR9 with the heavy chains of thrombin as predicted by PDBSum software. **C.** Contact-map analysis between the residues of ACR9 (vertical axis) and heavy chain of thrombin (horizontal axis) predicted by PDBsum server. Orange and violet colors represent non-bonded contact and hydrogen bond, respectively.

6.2.8.3 Docking of ACR9 with FXa

ACR9 also showed interaction with FXa (Fig 6.12A) via 4 H-bond and 43 non-bonded contacts (Fig 6.12B). Contact map analysis of docked ACR9 and FXa showed that 6 residues of ACR9 interacted with 10 residues of the heavy (D) chain of FXa (Fig 6.12C). The predicted ACE and GE of the interaction was determined at -39.86 and -23.93, respectively.

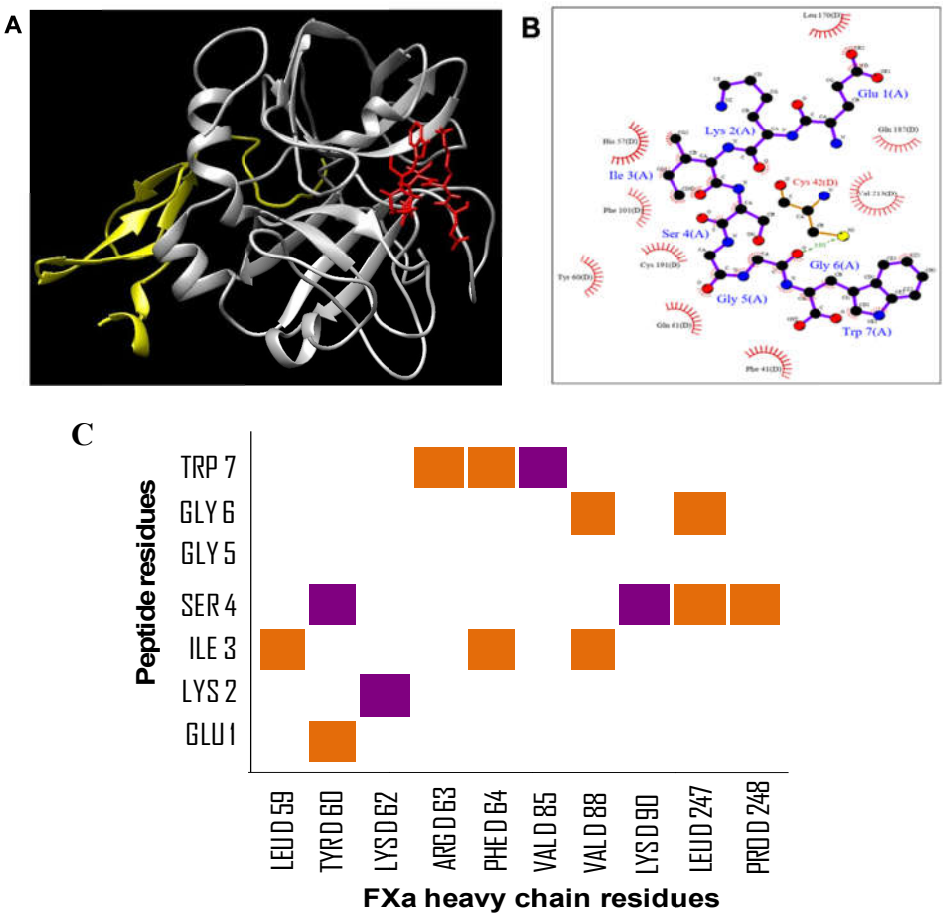

Fig 6.12. Docking of ACR9 with factor Xa. A. Best docking model of ACR9 with FXa (PDB ID: 1C5M) as predicted by the ClusPro 2.0 web server; red, grey, and yellow

chains represent ACR9, heavy (D) chain, and light (F) chain of FXa, respectively. **B.** Ligplot analysis to show the residue-to-residue interaction of ACR9 with the heavy chain of FXa predicted by PDBSum software. **C.** Contact-map analysis between the residues of ACR9 (vertical axis) and heavy chain of FXa (horizontal axis), as predicted by PDBsum server. Orange and violet colours represent non-bonded contact and hydrogen bond, respectively.

6.2.9. Determination of antigenicity of ACR9

As predicted by EMBOSS antigenic explorer, ACR9 was devoid of antigenicity with an average antigenic propensity score of 0.95.

6.2.10 Spectrofluorometry interaction of ACR9 with thrombin and FXa

6.2.10.1 Interaction with thrombin

ACR9 dose-dependently increased the fluorescence intensity of thrombin with emission maxima (λmax) at ~347 nm (Fig 6.13). The one site-specific binding curve showed that optimum increase in fluorescence intensity of thrombin occurred at 7.5 µM of ACR9 (Fig 6.13 inset).

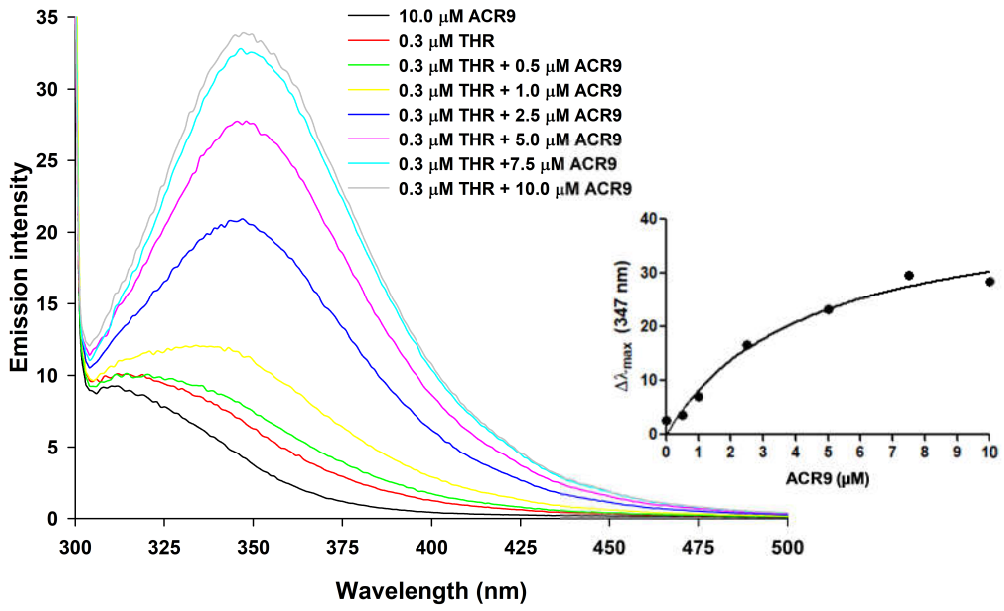

Fig 6.13. Spectrofluorometry analysis to determine the dose-dependent (0.5 – 10.0 µM) binding of ACR9 to thrombin (0.3 µM). **Inset:** One site-specific binding curves

showing the change in the maximum fluorescence intensity (Δλmax) of thrombin in presence of different concentrations of ACR9.

6.2.10.2 Interaction of ACR9 with FXa

ACR9 also dose-dependently enhanced the fluorescence intensity of FXa at ~345 nm (Fig 6.14); one site-specific binding curve showed progressive increase in fluorescence intensity of FXa in presence of ACR9 (Fig 6.14 inset).

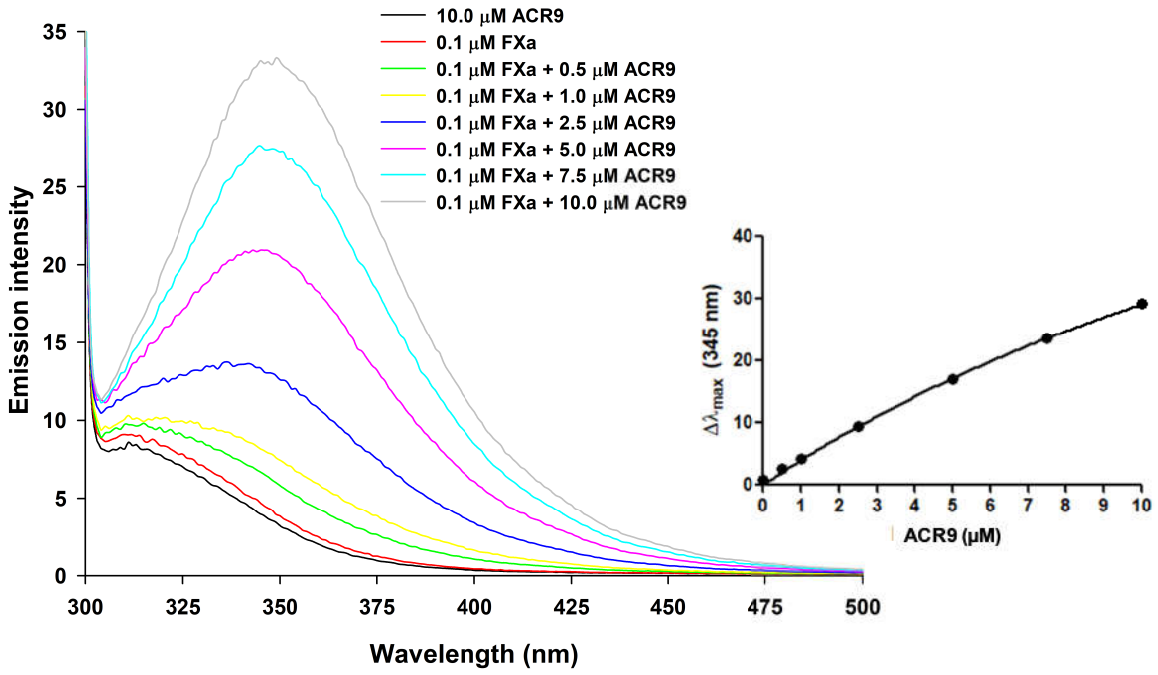

Fig 6.14. Spectrofluorometry analysis to determine the dose-dependent (0.5 – 10.0 µM) binding of ACR9 to FXa (0.1 µM). **Inset:** One site-specific binding curves showing the change in the maximum fluorescence intensity (Δλmax) of FXa in presence of different concentrations of ACR9.

6.2.11 Surface plasmon resonance (SPR) analysis to demonstrate binding of ACR9 to thrombin

The binding of the ACR9 with thrombin by SPR analysis showed that with an increase in the concentration of ACR9, its binding with thrombin was progressively enhanced (Fig 6.15) with a dissociation constant (K_D) of 3.8 ± 0.1 µM (Fig 6.15 inset).

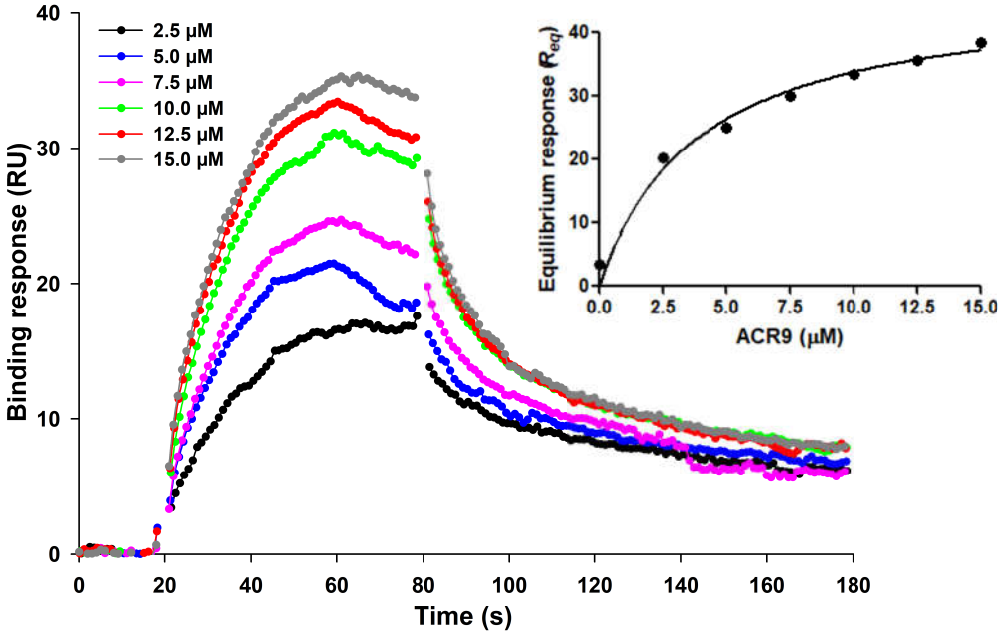

Fig 6.15. Binding sensogram depicting equilibrium binding of ACR9 (2.5 – 15.0 µM) with thrombin by surface plasmon resonance. Thrombin was immobilized on CM5 sensor chip at high density (~8000 RU) via amine coupling using a Biacore X100 (GE Healthcare, Freiburg, Germany). **Inset:** One-site saturation binding (peptide concentration vs R_{eq}) curve to calculate the K_D value of ACR9 for binding to thrombin as determined by SPR analysis.

6.2.12 *In vitro* cytotoxicity of ACR9

6.2.12.1 Effect of ACR9 on mammalian erythrocytes

Up to the tested dose of 5.0 µM, ACR9 did not exhibit any hemolytic activity of mammalian (goat) erythrocytes (Table 6.5).

Table 6.5. Assessment of dose-dependent (0. 5 – 5.0 µM) hemolytic activity of ACR9. The hemolytic activity was tested against 0.5% (v/v) mammalian washed erythrocytes suspension. Data represent mean ± S.D of triplicate experiments.

Samples	% hemolysis
1X PBS	0 (negative control)
1% Triton X-100	100 (positive control)
0.5 µM ACR9	0.98 ± 0.05

1.0 µM ACR9	0.74 ± 0.04
2.5 µM ACR9	1.17 ± 0.09
5.0 µM ACR9	2.99 ± 0.15

6.2.12.2 Effect of ACR9 on mammalian cells by MTT assay

The peptide was non-cytotoxic towards human embryonic kidney (HEK-293) and human breast adenocarcinoma (MCF-7) cells (Fig 6.16).

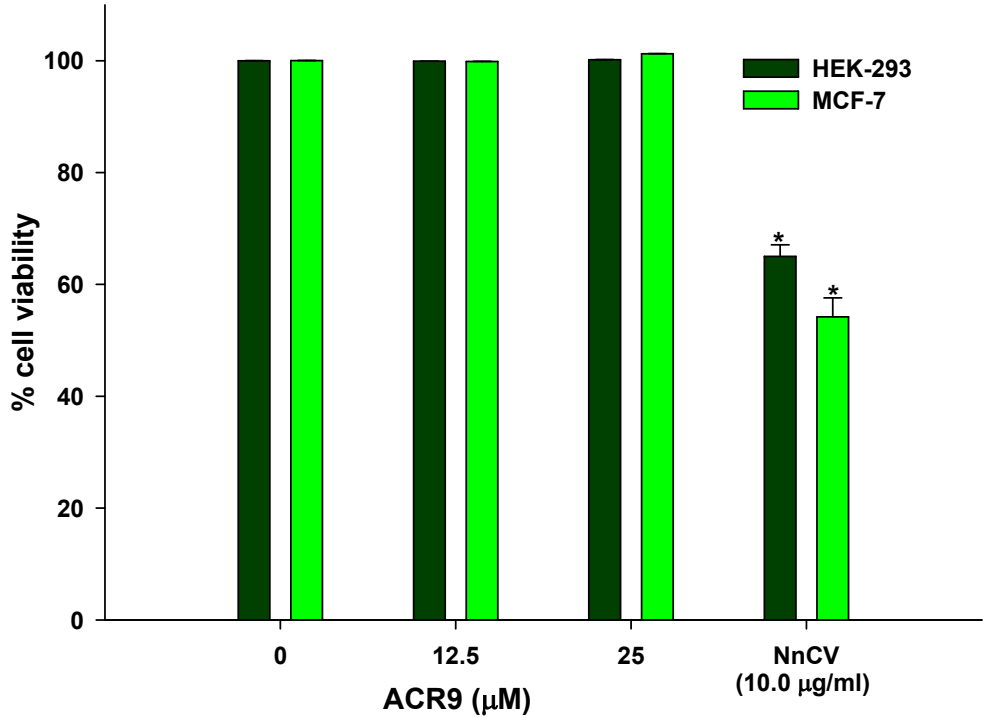

Fig 6.16. Cytotoxicity exhibited by ACR9 (12.5 and 25.0 µM) towards mammalian breast cancer cells (MCF-7) and human embryonic kidney cells (HEK-293). Values are mean ± SD of triplicate determinations.

6.2.12.3 Effect of ACR9 on cell cycle by flow cytometry analysis

Flow cytometry analysis of MCF-7 cells treated with ACR9 did not show significant difference ($p>0.05$) in G_1, S, and G_2 phases as compared to control cells suggesting it did not retard cell cycle of this mammalian cell (Fig 6.17).

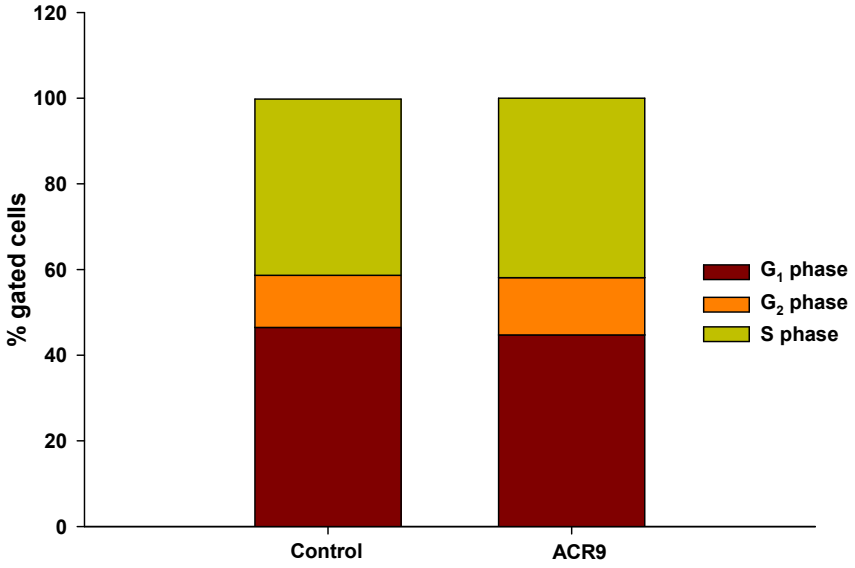

Fig 6.17. F**low cytometry analysis of cell cycle using propidium iodide (PI) staining.** The MCF-7 cells (1.5 × 10^5 cells per ml) were treated for 24 h at 37 ˚C, 5% CO_2 with ACR9 (10.0 µg/ml). Cells were harvested by trypsinization and stained with PI for 2 h and analyzed by flow cytometry. Values are mean ± SD of triplicate determinations.

6.2.13 Assessment of *in vivo* toxicity of ACR9

6.2.13.1 Effect on survival and behavioral parameters

The *in vivo* toxicity assessment demonstrated that at a dose of 4.0 mg/kg ACR9 was non-toxic to Wistar rats and did not show significant change ($p>0.05$) in the behavioral parameters of the treated group of rats as compared to control group of rats (Table 6.6A).

6.2.13.2 Effect on serological parameters

The serological parameters did not show any significant deviation ($p>0.05$) in treated rats as compared to the control group of rats (Table 6.6B).

6.2.13.3 Effect on blood parameters

Further, there was no any significant deviation ($p>0.05$) in hematological parameters of the treated rats as compared to the control group of rats (Table 6.6C).

Table 6.6A. Behavioral changes, if any, in Wistar rats (n=3 per group) after 72 h of intravenous injection of ACR9 (4.0 mg/kg dose). Values are mean ± SD of three (n=3 per group) independent determinations. Differences of values in each row are not significant ($p>0.05$).

Group of rats	Parameters									
	Body weight (g)		Grip strength (s)		Rectal temperature (F)		Fecal tendency (per 30 min)		Frequency of urination (per 30 min)	
	Initial*	Final¶	Initial*	Final¶	Initial*	Final¶	Initial*	Final¶	Initial*	Final¶
Control	140 ± 1.8	143 ± 2.1	49.5 ± 1.3	52.1 ± 0.9	95.1 ± 0.2	94.9 ± 1.6	5 ± 0.4	4 ± 0.7	4 ± 0.5	4 ± 0.8
ACR9-treated	145 ± 1.6	142 ± 2.0	46.9 ± 2.0	49.2 ± 1.4	93.8 ± 1.2	94.5 ± 1.6	5 ± 0.1	6 ± 0.2	5 ± 0.2	6 ± 0.5

*before injection; ¶after 72 h post injection

Table 6.6B. Effect of ACR9 (4.0 mg/kg) on the serum parameters of Wistar strain rats after 72 h of admistration (*i.v.*). Values are mean ± SD of three independent determinations. Differences of values in each row are not significant (p>0.05).

Parameter	Control	ACR9
Glucose (mg/dL)	49.00 ± 2.50	50.00 ± 2.50
SGPT	115.00 ± 5.80	111.00 ± 5.60
SGOT	18.00 ± 0.09	13.00 ± 0.70
Bilirubin (mg/dL)	0.25 ± 0.02	0.26 ± 0.01
Urea (mg/dL)	3.10 ± 0.02	2.80 ± 0.01
Uric acid (mg/dL)	1.69 ± 0.01	2.24 ± 0.01
Creatinine (mg/dL)	0.10 ± 0.01	0.10 ± 0.01
Triglyceride (mg/dL)	86.60 ± 4.30	73.09 ± 3.70
Cholesterol (mg/dL)	181.30 ± 9.10	154.70 ± 7.70
LDL (mg/dL)	78.60 ± 3.90	76.70 ± 3.80
HDL (mg/dL)	20.30 ± 1.00	19.30 ± 1.00
Total protein (mg/dL)	14.41 ± 0.70	14.73 ± 0.70

Table 6.6C. Effect of ACR9 (4.0 mg/kg) on the blood parameters of treated Wistar rats after 72 h of admistration (*i.v.*). Values are mean ± SD of three independent determinations. Differences of values in each row are not significant (p>0.05).

Parameter	Control	ACR9
WBC[a] (m/mm^3)	5.06 ± 0.33	5.14 ± 0.12
Lymphocytes (%)	36.17 ± 1.18	40.25 ± 2.10
Monocytes (%)	5.67 ± 0.90	6.19 ± 0.30

Neutrophils (%)	50.63 ± 2.25	42.97 ± 2.10
Eosinophils (%)	10.63 ± 0.15	9.95 ± 0.51
Basophils (%)	0.10 ± 0.01	0.14 ± 0.02
Total RBC[b] (m/mm^3)	8.77 ± 0.04	9.14 ± 0.50
MCV[c] (fl)	44.23 ± 1.22	49.58 ± 2.50
HCt[d] (%)	36.20 ± 1.80	35.10 ± 1.80
MCH[e] (pg)	15.77 ± 0.18	16.47 ± 0.80
MCHC[f] (g/dl)	37.13 ± 1.09	35.19 ± 1.81
RDW[g](%)	15.73 ± 1.06	11.98 ± 1.01
Hb[h] (g/dl)	12.70 ± 0.03	11.80 ± 0.16
MPV[i] (fl)	6.93 ± 0.16	7.08 ± 0.14
PCt[j] (%)	0.31 ± 0.01	0.29 ± 0.01
PDW[k](%)	8.37 ± 0.40	8.14 ± 0.60

[a] white blood corpuscles; [b]red blood corpuscles; [c]mean corpuscular volume expressed in femtolitre; [d]hematocrit value; [e]mean corpuscular hemoglobin expressed in picograms; [f]MCH concentration expressed in gram per deciliter; [g]red blood cell distribution width; [h]hemoglobin content expressed in gram per deciliter; [i]mean platelet volume in femtolitre; [j] platelet crit; [k] platelet distribution width.

6.2.13.4 Effect on histological parameters

Histological analysis of major tissues of ACR9-treated and untreated (control) animals did not exhibit any gross morphological difference (Fig 6.18) thereby suggesting ACR9 is devoid of toxicity in rodent.

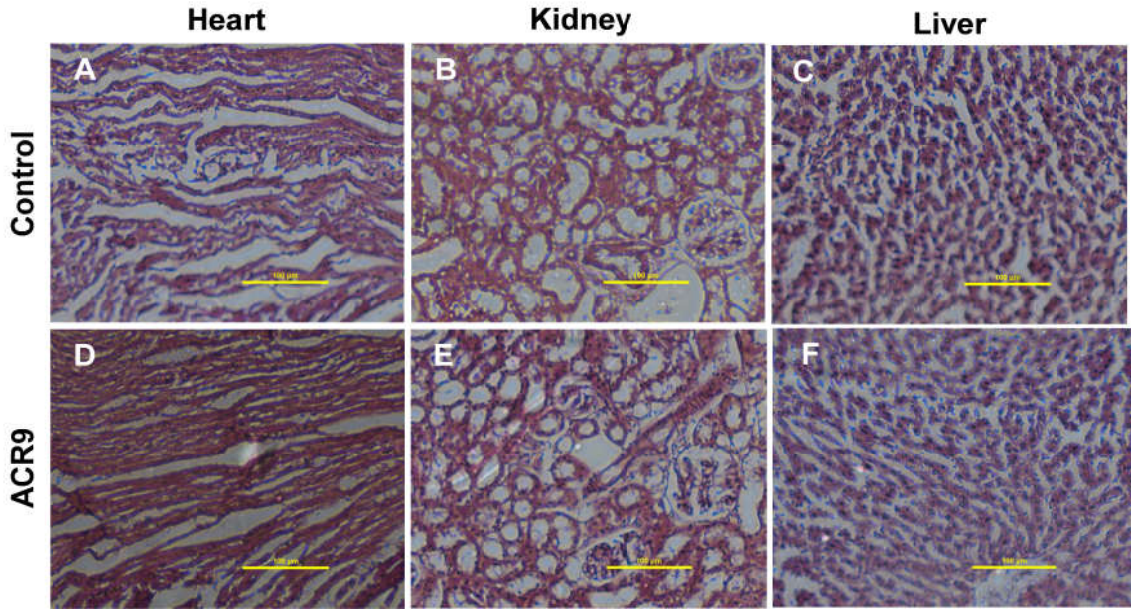

Fig 6.18. Histological images of heart, kidney, and liver tissues of Wistar strain rats treated with ACR9 (4.0 mg/kg) and control group of rats. The tissues were cut, fixed, dehydrated, and embedded in paraffin before sectioning, and stained with eosin-hematoxylin for histopathology study. Scale bar = 100 µm.

6.2.14 *In vivo* therapeutic property of ACR9

6.2.14.1 *In vivo* anticoagulant property of ACR9

ACR9 exhibited superior *in vivo* anticoagulant activity ($p<0.05$) as compared to argatroban and heparin under identical experimental conditions (Table 6.7). Nevertheless, ACR9 was devoid of *in vivo* and *ex vivo* defibrinogenation activity (Table 6.8).

6.2.14.2 *In vivo* antithrombotic property of ACR9

Pre-treatment of rats with ACR9 significantly ($p<0.05$) inhibited the κ-carrageenan-induced thrombus formation in the tails of rats (Fig 19A). Further, the anti-thrombotic potency of ACR9 was found to be higher than that of argatroban (Fig 19B).

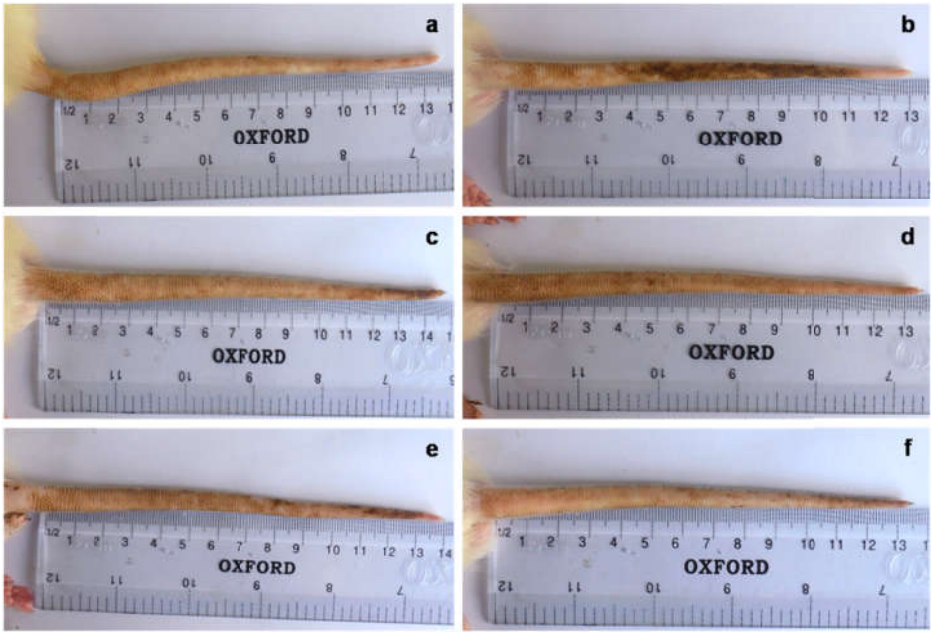

Fig 6.19A. Antithrombotic property of ACR9. Induction of thrombosis in tails of rats treated with 0.2 mg/kg and 0.4 mg/kg of argatroban and 7-mer peptide. Rats were treated intravenously with (a) 1X PBS, (b) 0.9 mg/kg κ-carrageenan, (c) 0.2 mg/kg and (d) 0.4 mg/kg argatroban followed by 0.9 mg/kg κ-carrageenan; (e) 0.2 mg/kg and (f) 0.4 mg/kg ACR9 followed by 0.9 mg/kg κ-carrageenan.

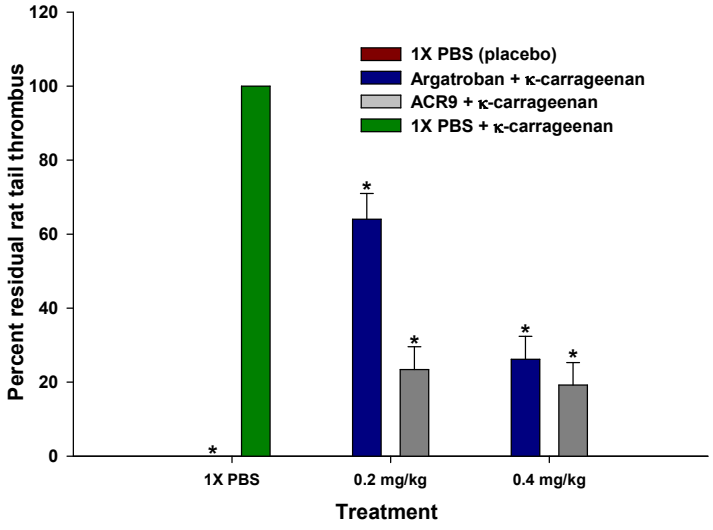

Fig 6.19B. Percent thrombus formation in the tails of Wistar rats (n=4) after 48 h of intravenous administration of 0.9 mg/kg κ-carrageenan in untreated (control), ACR9, and argatroban-treated rats. Values are mean ± SD of four animals per group. Significance of difference with respect to control (100%), *p<0.05.

Table 6.7. Comparison of i*n vivo* anticoagulant activity of ACR9, argatroban, and heparin post 60 min of administration (*i.v.*) in Wistar strain rats. Values are mean ± SD of six independent determinations. Significance of difference *p<0.01 as compared to control, and ¶p<0.05 as compared to argatroban.

Sample	PT (s)	INR[a]	APTT (s)	INR	TT (s)	Ca^{2+} clotting time (s)	Tail bleeding time (s)
Control	17.20 ± 0.4	1.00	30.32 ± 0.1	1.00	63.01 ± 0.1	79.93 ± 1.9	61.11 ± 5.3
ACR9 (0.4 mg/kg)	38.13 ± 1.1*¶	2.22	39.61 ± 0.7*	1.31	124.18 ± 5.8*¶	246.94 ± 8.8*¶	206.40 ± 10.6*¶
Argatroban (0.4 mg/kg)	27.81 ± 0.8*	1.62	37.91 ± 0.4*	1.25	106.18 ± 0.6*	107.43 ± 2.8*	154.56 ± 10.2*
Heparin (0.4 mg/kg)	23.84 ± 0.6*¶	1.39	34.73 ± 1.0	1.15	93.22 ± 3.7*	97.48 ± 2.9*	120.13 ± 6.5*¶

[a] international normalized ratio (INR) = Value of treated sample / value of control

Table 6.8. Effect of 0.4 mg/kg ACR9 on defibrinogenation activity after 60 min of administration (*i.v.*). The Lunathrombase was used as a positive control. Values are mean ± SD of three independent determinations. Significance of difference, *p<0.05 with respect to control.

ACR9 (mg/kg)	Blood plasma fibrinogen level (mg/ml)	
	***In vivo* (PPP from ACR9 treated / control Wistar strain rats)**	***Ex vivo* (PPP from untreated Wistar strain rats)**
Control	2.49 ± 0.22	2.62 ± 0.17
0.4 mg/kg ACR9	2.51 ± 0.19	2.52 ± 0.14
0.4 mg/kg Lunathrombase‡	1.48 ± 0.08*	1.29 ± 0.12*

‡A fibrinogenolytic enzyme isolated from leave extract of *Leucas indica* [15].

6.3 Discussion

The non-toxic anticoagulant PLA_2 enzyme ($NnPLA_2$-I) from *N. naja* venom exerts its anticoagulant activity via catalytic (phospholipids hydrolysis) activity and partly by non-enzymatic inhibition of thrombin (see chapter IV). Apart from the catalytic site, snake venom PLA_2s possess an additional target-specific pharmacological site (residues 54 – 77) responsible for determining the pathophysiological activity of this enzyme [13].

The 7-mer peptide (ACR9) developed from the pharmacological site of $NnPLA_2$-I prolonged the prothrombin time (PT) and thrombin time (TT) of PPP, thereby suggesting that it affects the extrinsic and / or common pathway of the blood coagulation cascade [16,17]. Further, the *in vitro* result showing greater inhibition of thrombin compared to FXa by ACR9 is well corroborated with *in silico* analysis results. Interestingly some of the ACR peptides (1, 2, 5, and 6) showed higher ACE with thrombin (Table 6.1); nevertheless, they failed to elicit a significant anticoagulant activity in *in vitro* conditions suggesting that perhaps the smaller length of the ACR9 enhances its flexibility to exhibit strongest inhibition of the coagulation factors. The docking study showed (predicted) that ACR9 in addition to binding to active site may also bind to some other site of thrombin those results in mixed mode of thrombin

inhibition. However, ACR9 does not interact with the active site of FXa and demonstrates uncompetitive mode of FXa inhibition. These data indicate that ACR9 binds to FXa when it forms an enzyme-substrate complex with prothrombin and it does not bind to free substrate (prothrombin) [18]. Further, the results of the docking studies showing greater interaction (lower atomic contact energy) of ACR9 with thrombin compared to FXa was also supported by *in vitro* study showing higher inhibition of thrombin compared to FXa by ACR9; interestingly, $NnPLA_2$-I did not show FXa inhibition (see section 4.2.7.2.4). It may be reasonable to anticipate that relatively much smaller size and lesser steric hindrance of ACR9 compared to $NnPLA_2$-I could possibly aid in binding of this peptide to different sites of FXa thereby leading to an uncompetitive inhibition of this key coagulation factor.

In contrast to low molecular mass (<5 kDa) thrombin and FXa inhibitors derived from hematophagous insects [19-22], snake venom serine protease inhibitors are usually higher molecular mass proteins / peptides (6 – 29 kDa) [23-26]; the only exception is the Ruviprase (4.4 kDa) isolated from *Daboia russelii* venom [2]. Further, a novel bioactive peptide (ACH-11) with the sequence LTFPRIVFVLG was derived from hydrolysates of *Agkistrodon acutus* venom that exhibited FXa inhibition and antiplatelet property [10]. The 'hirulogs', which are ~20 amino acid long synthetic peptides synthesized from the C-terminal region of hirudin [11,27], show thrombin inhibition by binding to a site on thrombin other than its active site suggesting non-competitive inhibition of thrombin [27]. However, argatroban shows only competitive mode of thrombin inhibition [28,29]. In a sharp contrast, ACR9 is capable of binding to the catalytic site as well as to some other sites of thrombin indicating differences in the mechanism of thrombin inhibition by ACR9, hirulogs, and argatroban.

To reduce the number of test compounds, the *in silico* or virtual analysis of ligand-target molecule interaction has gained a tremendous momentum in pharmaceutical industry and a set of molecules / compounds showing best interactions with the target molecule are further considered for *in vitro* analysis [30,31]. However, *in silico* studies are prediction only; therefore, validation of *in silico* results by wet lab experiments is the indispensable prerequisite for successful development of drug prototypes. Spectrofluorometry analysis is one of the primary techniques to measure the

interaction between proteins [32,33]. The increase in the fluorescence intensity of thrombin and FXa post addition of ACR9 validated their interactions with ACR9 [33]. Further, K_D value of ACR9 towards thrombin is significantly lower than that of argatroban (53.8 μM) [34].

The transition of anticoagulant drugs from high molecular weight compounds such as unfractionated heparin (UFH), hirudin, and warfarin to low molecular weight heparin (LMWH), hirulogs, and smaller molecules such as argatroban and dabigatran was due to several adverse pharmacological effects of former group of drugs [1,35]. Nevertheless, low molecular mass peptides have certain potential advantages over chemical molecules as anticoagulant drugs [2,6,10,36,37]. Notably, low molecular mass peptides as compared to low molecular weight synthetic drugs possess higher affinity towards their target, have lower toxicity, and have high tissue penetration ability [36], albeit some complications are also associated with low-molecular mass peptides [36,37]. However, several strategies have been developed in recent years to overcome such limitations [36].

Rats (Wistar strain) share approximately 90% similarity with the human genome [38], thus making them one of the most widely used animal models in medical research [39]. Administration of ACR9 at a dose of 4.0 mg/kg, which is approximately 20 times greater than the minimum *in vivo* antithrombotic dose of this peptide (0.2 mg/kg; Figs 19A,B), did not show adverse pharmacological effects and acute toxicity in treated rats thereby suggesting its pre-clinical safety and higher therapeutic index. Further, the optimum INR (international normalized ratio) value of PT and APTT suggested that ACR9 may not produce the risk of internal bleeding disorder [40]. The *in silico* analysis indicated non-antigenic nature of ACR9 suggesting adverse immunological response in patients following prolong application of this molecule is unlikely; nevertheless, it needs to be validated by chronic toxicity study in rodents.

Bibliography

[1] Hirsh, J., O'Donnell, M., and Weitz, J. I. New anticoagulants. *Blood*, 105(2): 453-463, 2005.

[2] Thakur, R., Kumar, A., Bose, B., Panda, D., Saikia, D., Chattopadhyay, P., and Mukherjee, A. K. A new peptide (Ruviprase) purified from the venom of *Daboia russelii russelii* shows potent anticoagulant activity via non-enzymatic inhibition of thrombin and factor Xa. *Biochimie*, 105: 149-158, 2014.

[3] Esmon, C. T. Targeting factor Xa and thrombin: impact on coagulation and beyond. *Thrombosis and Haemostasis*, 111(4): 625-633, 2014.

[4] Kini, R. M. Anticoagulant proteins from snake venoms: structure, function and mechanism. *Biochemical Journal*, 397(3): 377-387, 2006.

[5] Chan, Y. S., Cheung, R. C., Xia, L., Wong, J. H., Ng, T. B., and Chan, W. Y. Snake venom toxins: toxicity and medicinal applications. *Applied Microbiology and Biotechnology*, 100(14): 6165-6181, 2016.

[6] Craik, D. J., Fairlie, D. P., Liras, S., and Price, D. The future of peptide-based drugs. *Chemical Biology & Drug Design*, 81(1): 136-147, 2013.

[7] Kaspar, A. A. and Reichert, J. M. Future directions for peptide therapeutics development. *Drug Discovery Today*, 18(17-18): 807-817, 2013.

[8] Lau, J. L. and Dunn, M. K. Therapeutic peptides: Historical perspectives, current development trends, and future directions. *Bioorganic & Medicinal Chemistry*, 26(10): 2700-2707, 2018.

[9] Pennington, M. W., Czerwinski, A., and Norton, R. S. Peptide therapeutics from venom: Current status and potential. *Bioorganic & Medicinal Chemistry*, 26(10): 2738-2758, 2018.

[10] Chen, M., Ye, X., Ming, X., Chen, Y., Wang, Y., Su, X., Su, W., and Kong, Y. A Novel direct dactor Xa inhibitory peptide with anti-platelet aggregation activity from *Agkistrodon acutus* venom hydrolysates. *Scientific Reports*, 5: 10846, 2015.

[11] Maraganore, J. M., Chao, B., Joseph, M. L., Jablonski, J., and Ramachandran, K. L. Anticoagulant activity of synthetic hirudin peptides. *Journal of Biological Chemistry*, 264(15): 8692-8698, 1989.

[12] De Groot, A. S. and Scott, D. W. Immunogenicity of protein therapeutics. *Trends in Immunology*, 28(11): 482-490, 2007.

[13] Kini, R. M. and Evans, H. J. Structure-function relationships of phospholipases. The anticoagulant region of phospholipases A_2. *Journal of Biological Chemistry*, 262(30): 14402-14407, 1987.

[14] Kini, R. M. Excitement ahead: structure, function and mechanism of snake venom phospholipase A_2 enzymes. *Toxicon*, 42(8): 827-840, 2003.

[15] Gogoi, D., Arora, N., Kalita, B., Sarma, R., Islam, T., Ghosh, S. S., Devi, R., and Mukherjee, A. K. Anticoagulant mechanism, pharmacological activity, and assessment of preclinical safety of a novel fibrin(ogen)olytic serine protease from leaves of *Leucas indica*. *Scientific Reports*, 8(1): 6210, 2018.

[16] Kamal, A. H., Tefferi, A., and Pruthi, R. K. How to interpret and pursue an abnormal prothrombin time, activated partial thromboplastin time, and bleeding time in adults. *Mayo Clinic Proceedings*, 82(7): 864-873, 2007.

[17] Dahlbäck, B. Blood coagulation. *The Lancet*, 355(9215): 1627-1632, 2000.

[18] Dougall, I. G. and Unitt, J. Evaluation of the biological activity of compounds: techniques and mechanism of action studies. In Wermuth, C. G., Aldous, D., Raboisson, P., Rognan, D, editors, *The Practice of Medicinal Chemistry*, pages 15-43. Academic Press, Elsevier Inc., Massachusetts, CA, 2015.

[19] Cappello, M., Bergum, P. W., Vlasuk, G. P., Furmidge, B. A., Pritchard, D. I., and Aksoy, S. Isolation and characterization of the tsetse thrombin inhibitor: a potent antithrombotic peptide from the saliva of *Glossina morsitans morsitans*. *American Journal of Tropical Medicine and Hygiene*, 54(5): 475-480, 1996.

[20] Ciprandi, A., de Oliveira, S. K., Masuda, A., Horn, F., and Termignoni, C. *Boophilus microplus*: its saliva contains microphilin, a small thrombin inhibitor. *Experimental Parasitology*, 114(1): 40-46, 2006.

[21] Koh, C. Y., Kazimirova, M., Trimnell, A., Takac, P., Labuda, M., Nuttall, P. A., and Kini, R. M. Variegin, a novel fast and tight binding thrombin inhibitor from

the tropical bont tick. *Journal of Biological Chemistry*, 282(40): 29101-29113, 2007.

[22] Waxman, L., Smith, D. E., Arcuri, K. E., and Vlasuk, G. P. Tick anticoagulant peptide (TAP) is a novel inhibitor of blood coagulation factor Xa. *Science*, 248(4955): 593-596, 1990.

[23] Zingali, R. B., Jandrot-Perrus, M., Guillin, M. C., and Bon, C. Bothrojaracin, a new thrombin inhibitor isolated from *Bothrops jararaca* venom: characterization and mechanism of thrombin inhibition. *Biochemistry*, 32(40): 10794-10802, 1993.

[24] Osipov, A. V., Filkin, S. Y., Makarova, Y. V., Tsetlin, V. I., and Utkin, Y. N. A new type of thrombin inhibitor, noncytotoxic phospholipase A_2, from the *Naja haje* cobra venom. *Toxicon*, 55(2-3): 186-194, 2010.

[25] Mukherjee, A. K., Kalita, B., and Thakur, R. Two acidic, anticoagulant PLA_2 isoenzymes purified from the venom of monocled cobra *Naja kaouthia* exhibit different potency to inhibit thrombin and factor Xa via phospholipids independent, non-enzymatic mechanism. *PloS One*, 9(8): e101334, 2014.

[26] Mukherjee, A. K., Mackessy, S. P., and Dutta, S. Characterization of a Kunitz-type protease inhibitor peptide (Rusvikunin) purified from *Daboia russelii russelii* venom. *International Journal of Biological Macromolecules*, 67: 154-162, 2014.

[27] Maraganore, J. M. and Fenton, J. W., 2nd. Thrombin inhibition by synthetic hirudin peptides. *Advances in Experimental Medicine and Biology*, 281: 177-183, 1990.

[28] Cossy, J. and Belotti, D. A short synthesis of argatroban. a potent selective thrombin inhibitor. *Bioorganic & Medicinal Chemistry Letters*, 11(15): 1989-1992, 2001.

[29] Matsuo, T., Koide, M., and Kario, K. Development of argatroban, a direct thrombin inhibitor, and its clinical application. *Seminars in Thrombosis and Hemostasis*, 23(6): 517-522, 1997.

[30] Terstappen, G. C. and Reggiani, A. *In silico* research in drug discovery. *Trends in Pharmacological Sciences*, 22(1): 23-26, 2001.

[31] Koutsoukas, A., Simms, B., Kirchmair, J., Bond, P. J., Whitmore, A. V., Zimmer, S., Young, M. P., Jenkins, J. L., Glick, M., Glen, R. C., and Bender, A. From *in silico* target prediction to multi-target drug design: current databases, methods and applications. *Journal of Proteomics*, 74(12): 2554-2574, 2011.

[32] Saikia, D., Thakur, R., and Mukherjee, A. K. An acidic phospholipase A_2 (RVVA-PLA_2-I) purified from *Daboia russelli* venom exerts its anticoagulant activity by enzymatic hydrolysis of plasma phospholipids and by non-enzymatic inhibition of factor Xa in a phospholipids/Ca^{2+} independent manner. *Toxicon*, 57(6): 841-850, 2011.

[33] Mukherjee, A. K., Dutta, S., Kalita, B., Jha, D. K., Deb, P., and Mackessy, S. P. Structural and functional characterization of complex formation between two Kunitz-type serine protease inhibitors from Russell's Viper venom. *Biochimie*, 128-129: 138-147, 2016.

[34] Wang, X., Zhang, Y., Yang, Y., Wu, X., Fan, H., and Qiao, Y. Identification of berberine as a direct thrombin inhibitor from traditional Chinese medicine through structural, functional and binding studies. *Scientific Reports*, 7: 44040, 2017.

[35] Bircher, A. J., Harr, T., Hohenstein, L., and Tsakiris, D. A. Hypersensitivity reactions to anticoagulant drugs: diagnosis and management options. *Allergy*, 61(12): 1432-1440, 2006.

[36] Sato, A. K., Viswanathan, M., Kent, R. B., and Wood, C. R. Therapeutic peptides: technological advances driving peptides into development. *Current Opinion in Biotechnology*, 17(6): 638-642, 2006.

[37] Sun, L. Peptide-based drug development. *Modern Chemistry and Applications*, 1(1): 1-2, 2013.

[38] Mullins, L. J. and Mullins, J. J. Insights from the rat genome sequence. *Genome Biology*, 5(5): 221, 2004.

[39] Iannaccone, P. M. and Jacob, H. J. Rats! *Disease Models & Mechanisms*, 2(5-6): 206-210, 2009.

[40] Horstkotte, D., Schulte, H. D., Bircks, W., and Strauer, B. E. Lower intensity anticoagulation therapy results in lower complication rates with the St. Jude Medical prosthesis. *Journal of Thoracic and Cardiovascular Surgery*, 107(4): 1136-1145, 1994.